



Develop the Hybrid Empirical Mode Decomposition with Fast Mask CNN to Improve the Performance Measures of PCG Signals



Suganthi Brindha Gnanapirakasam* , J. Manjula 

Department of Electronics and Communication Engineering, College of Engineering and Technology, SRM Institute of Science and Technology, Kattankulathur, Chennai 603203, Tamil Nadu, India

Corresponding Author Email: suganthg@srmist.edu.in

Copyright: ©2024 The authors. This article is published by IETA and is licensed under the CC BY 4.0 license (<http://creativecommons.org/licenses/by/4.0/>).

<https://doi.org/10.18280/ts.410418>

ABSTRACT

Received: 1 December 2023

Revised: 6 March 2024

Accepted: 7 April 2024

Available online: 31 August 2024

Keywords:

Cardiovascular Diseases (CVD), denoising, double density discrete wavelet transform, Empirical Mode Decomposition (EMD), faster mask convolutional neural network, Mean Square Error (MSE), phonocardiogram, Signal-to-Noise Ratio (SNR)

The Phonocardiogram (PCG) signal provides crucial insights into heart function and is instrumental in identifying cardiac dysfunctions leading to heart failure. Given the significant impact of Cardiovascular Diseases (CVD) on human life and socioeconomic conditions, early detection of cardiac problems is imperative. This study evaluates a hybrid denoising technique, Empirical Mode Decomposition (EMD) with Fast Mask Convolutional Neural Network (EMD-FMCNN), to reduce the impact of noise on PCG signals. Using datasets from the NHS supplemented with Additive White Gaussian Noise (AWGN), the effectiveness of the EMD-FMCNN approach is compared to the Double-Density Discrete Wavelet Transform (DD-DWT) methodology. Evaluation metrics such as Mean Square Error (MSE) and Signal-to-Noise Ratio (SNR) are utilized. The results indicate that the EMD-FMCNN approach outperforms DD-DWT, yielding superior SNR values of 25.55 dB compared to 18.19 dB, and achieving optimal MSE values of 0.01% compared to 0.42% for DD-DWT. The findings demonstrate the effectiveness of the EMD-FMCNN approach in denoising PCG signals, offering a promising method for improving the accuracy of cardiovascular disease diagnosis.

1. INTRODUCTION

Any mechanical process generates sound, and the heartbeat produces sound as well this sound could be audible or above depending on the sort of activity. Heart sounds in the auditory range originate from the mechanical actions of the heart brought on by its normal function [1]. It necessitates extra preparations, such as a stethoscope that operates on the resonant of the air column connected to the stethoscope's concept. However, signals could be digitally captured for later use and further analyzed with the help of the right electrical circuits [2]. The design and operation of the heart, the significance, source, and characteristics of the Hybrid Spatial Spectra (HSS) signals and murmurs produced, and the challenges associated with signal analysis.

The heart is the primary organ responsible for pumping blood through the circulatory system and into the various parts of the human body. The term CVD refers to illnesses that impact the blood vessels or the human heart [3]. Nearly 17.5 million deaths were attributed to CVDs in 2016, making them the top reason for death world. The lowest rate of CVD mortality effect could be achieved through early observation. There are many non-invasive techniques for diagnosing CVDs that rely on the electrical, mechanical, or magnetic activity of the heart [4]. Electrocardiograms (ECGs) are electrical heart activity, and tomography scans that were magnetic heart activity, were both frequently used to identify CVDs, but both have drawbacks due to their expensive nature and need for

specialized knowledge. Auscultation is a different way to identify cardiac illness and was recently given the label PCG. It was invented in the eighteenth century and simply requires a stethoscope as a diagnostic tool. The auscultation method, which was first described [5], is frequently used as the main indicator for human physiology, particularly cardiac activity, although it is mostly reliant on the clinical professional's skill to perceive and understand heart-generated sound.

The most accurate graphical depictions of heartbeats and murmurs (abnormal heartbeats) are obtained through PCG. S2, S1, S4, and S3, are the four heart sound components included in the PCG recording. In a normal heart, S4 and S3 heart sounds could also be detected in S2 and S1, which are produced by regular valve closure and opening in a healthy heart. S2 comes immediately after S3 and S4 comes right before S1. Heart rate monitoring, the detection of murmurs, and typical heart sounds are all performed using PCG signals [6].

PCG is a valuable diagnostic tool in the realm of CVD assessment, providing critical insights into the functioning of the heart through the analysis of its acoustic signatures. This non-invasive technique involves the recording and analysis of sounds produced by the heart and blood flow using specialized sensors placed on the chest. These sensors detect and amplify the mechanical vibrations generated by the heart's various activities, including the opening and closing of heart valves, turbulent blood flow, and abnormal heart sounds indicative of underlying cardiac conditions.

In the context of CVD, PCG serves as an indispensable tool for early detection, diagnosis, and monitoring of various cardiac abnormalities. By analyzing the frequency, intensity, timing, and duration of heart sounds, clinicians can identify anomalies such as murmurs, gallops, and clicks, which may signify structural defects, valve disorders, or hemodynamic abnormalities within the heart. Furthermore, PCG aids in distinguishing between benign and pathological heart sounds, guiding clinicians in making informed decisions regarding further diagnostic evaluations and appropriate treatment strategies for patients with suspected or established cardiovascular conditions.

The integration of advanced signal processing algorithms and machine learning techniques has enhanced the diagnostic accuracy and predictive capabilities of PCG in CVD management. By leveraging artificial intelligence and pattern recognition algorithms, researchers have developed automated systems capable of detecting subtle abnormalities in heart sounds, thereby facilitating rapid and accurate diagnosis of various cardiac pathologies. Moreover, the portability and cost-effectiveness of PCG devices make them ideal for widespread deployment in diverse healthcare settings, enabling timely screening, early intervention, and continuous monitoring of patients at risk for cardiovascular disease.

1.1 Characteristics of PCG signal

The first systolic is the longest and deepest and starts at the identical period to the R wave's climax, followed by the third proto-diastolic, the fourth presystolic, and the second diastolic. These four fundamental noises were identified in the typical cardiac cycle. The first two noises are critical to identifying the initial cardiac cycle and calculating heart rate. The S1 and S2 peaks' locations are very important for the correct diagnosis statement since the distance through the two peaks differentiates S1 to S2 (occasionally S2 can have a bigger amplitude than S1). Various cardiovascular conditions, such as damage to aortic stenosis, tricuspid or aorta insufficiency, the ventricular septum, mitral or pulmonary artery, can result in sound murmurs, which can occasionally contaminate this interval. Murmurs are noise-like sounds that have a frequency of up to 600 Hz and become more apparent when blood flow is accelerated across anomalies like obstructions or narrowing. The detection of the murmurs is crucial for determining the cause of the illness, even though they appear to be a noise element [7].

1.2 PCG artifacts

External or internal (physiological) noise sources have the potential to corrupt PCG readings. The following artifacts are the most significant sources of PCG signal disturbances: background music or speech, sensor movement, breathing sound, doors closing and other environmental noise, cough, and acoustic reducing of the bones and other problems. Electromagnetic waves could also be present in the measured signal [8] depending on how the sensor and electric storage elements are connected electrically.

Artifacts to PCG transmissions are an indicator of issues of interference and the intended PCG signal overlapping in a frequency band. A digital filter could be used to minimize high-frequency sound, including the well-known Butterworth band-pass filter, but the actual issue is the noise that is mixed in with the pure PCG signal using the identical frequency [9].

More advanced techniques, like Empirical Mode Decomposition (EMD) and wavelet Transform (WT), are frequently used to get clear of the artifact. Both approaches are frequently used in the evaluation of biological signals and PCGs, according to much research. The contrast of these two techniques for eliminating interference from PCG signals is the focus of the paper [10].

PCG signal was a noise issue that degraded the signal. Numerous elements and noise, such as electromagnetic fields from the surroundings, power frequency fluctuations, interaction with respiratory and digestive sounds, and electrical impulses from the human body, frequently obstruct the recording of heart sounds [11]. As a result, a suitable technique, to the EMD technique and a wavelet-based technique was needed to eliminate noise from PCG signals. PCG signals could be denoised using the EMD approach, which is useful for data processing, particularly for nonlinear signals and non-stationary. Intrinsic Mode Function (IMF) was an oscillation element that could be separated from the PCG signal during the denoising method using the EMD approach [12]. A wavelet-based denoising system, like the DD-DWT also employed a decomposition technique to extract the data signal from the sound.

The EMD approach was utilized to denoise an ECG signal with SNR and MSE serving as performance indicators. Work utilized MSE and SNR parameters to precision the denoising method efficiency of the PCG signal. The EMD approach was also used to separate a signal from a lot of noise signals. Boudraa contrasts the outcomes with a denoising approach to wavelets. They evaluated the EMD outcome of the wavelet method using adaptable white Gaussian noise [13]. The PCG signal could be used to perform the wavelet-based denoising technique. Executed a DD-DWT to eliminate the EEG signal or claimed that it might be applied to denoise PCG or ECG, two additional bio signal types. The S1 and S2 of the phonocardiogram were identified via character extraction by Gadde and Kumar [14] using wavelet packet transforms utilized in a separate WT. Since Jaros et al. [15] demonstrated to application of DD-DWT to improve the signal and image, we employed DD-DWT to remove the PCG signal in our work and contrasted the outcome to the EMD approach [16]. To eliminate noise from the PCG signal, we proposed the EMD-FMCNN and DD-DWT methods using prior research.

1.3 Problem statement

The problem statement about PCG in the context of CVD revolves around the need for an efficient and reliable diagnostic tool that can accurately detect, diagnose, and monitor various cardiac abnormalities. Despite advancements in medical technology, Cardiovascular Diseases remain a leading cause of morbidity and mortality worldwide. Early detection and intervention are crucial for improving patient outcomes and reducing the burden of CVD on healthcare systems.

Current diagnostic modalities, while effective, often require specialized equipment, and trained personnel, and can be costly and time-consuming. This poses challenges, especially in resource-limited settings where access to advanced healthcare facilities may be limited. Additionally, the interpretation of traditional diagnostic tests such as echocardiography and electrocardiography can be subjective and may lack sensitivity in detecting subtle cardiac abnormalities.

PCG presents a promising solution to these challenges by offering a non-invasive, cost-effective, and portable method for assessing cardiac function. However, the widespread adoption and optimization of PCG in clinical practice are hindered by various factors, including the need for standardized recording and analysis protocols, the development of robust signal processing algorithms for automated detection of cardiac abnormalities, and the integration of PCG data into existing healthcare infrastructure for seamless patient management. Addressing these challenges will contribute to the advancement of PCG as a valuable tool in the diagnosis and management of cardiovascular disease, ultimately improving patient outcomes and healthcare delivery.

1.4 Limitations

Phonocardiogram (PCG) technology presents a promising avenue for diagnosing and managing cardiovascular disease (CVD), yet it comes with notable limitations. One significant challenge lies in the interpretation of PCG recordings, which demands specialized expertise to differentiate between normal and abnormal heart sounds accurately. Variability in individual heart sounds and external factors such as patient positioning and ambient noise further complicate interpretation, potentially leading to diagnostic inaccuracies. Additionally, technical factors such as sensor placement and equipment characteristics can introduce variability in the quality of PCG recordings, necessitating standardized protocols and advanced signal processing techniques to mitigate these challenges. Despite its potential, the clinical evidence supporting the diagnostic accuracy and prognostic value of PCG in CVD is still limited compared to established modalities like echocardiography, highlighting the need for large-scale clinical studies to validate its utility.

1.5 Motivations

Furthermore, the accessibility and affordability of PCG devices pose barriers to widespread adoption, particularly in resource-constrained healthcare settings. While PCG offers the advantages of non-invasiveness and portability, cost-effective solutions and integration strategies are essential to ensure equitable access to this diagnostic tool. Addressing these limitations through continued research, technological innovation, and healthcare system integration will be crucial for maximizing the potential of PCG in the diagnosis, management, and prevention of cardiovascular disease, ultimately improving patient outcomes and healthcare delivery.

The remainder of the section is as follows: Section 2 describes a brief about the signal and noise generation; wavelet transform and Empirical Mode Decomposition which is related to PCG. Section 3 states the proposed system and to design of the model of the system. Section 4 states the experimental findings and outcomes of the proposed system and section 5 concludes it.

2. RELATED WORKS

Two filtering techniques—EMD and WT—were developed in the MATLAB software for the PCG signal processing. The work focuses on removing speech signals, motion artifacts, and environmental noise from PCG data, which are the three

types of disturbance that emerge most frequently [17].

2.1 Signal and noise generation

To assess the effectiveness of the technique, PCG recordings of the Physio Bank and Think Lab's biological signal databases were employed. To demonstrate the efficacy of techniques in various PCG frequency categories, 2 physiological signals (further phy2 and phy1) and 2 pathological signals (signal of the hypertrophic cardiomyopathy, additional pat2, or systolic murmurs combined of a prosthetic mitral valve signal, additional pat1) were chosen. PCG signal individually, the following three types of interference were introduced (Figure 1): Sound artifacts from ecosystems and the patient's body represented by High Frequency (HF) [18] sound of a frequency method above 20 Hz (artificially created); possibly, some electromagnetic disturbance;

- Low-frequency (LF) noise that was artificially produced and a frequency level up to 100 Hz, replicating motion artifacts that mostly result in the movement of the detector to the person's chest.

- The Whole Frequency (WF) sound replicates ambient speech noise by combining a variety of voice waveforms (accessible from the Physio Bank dataset).

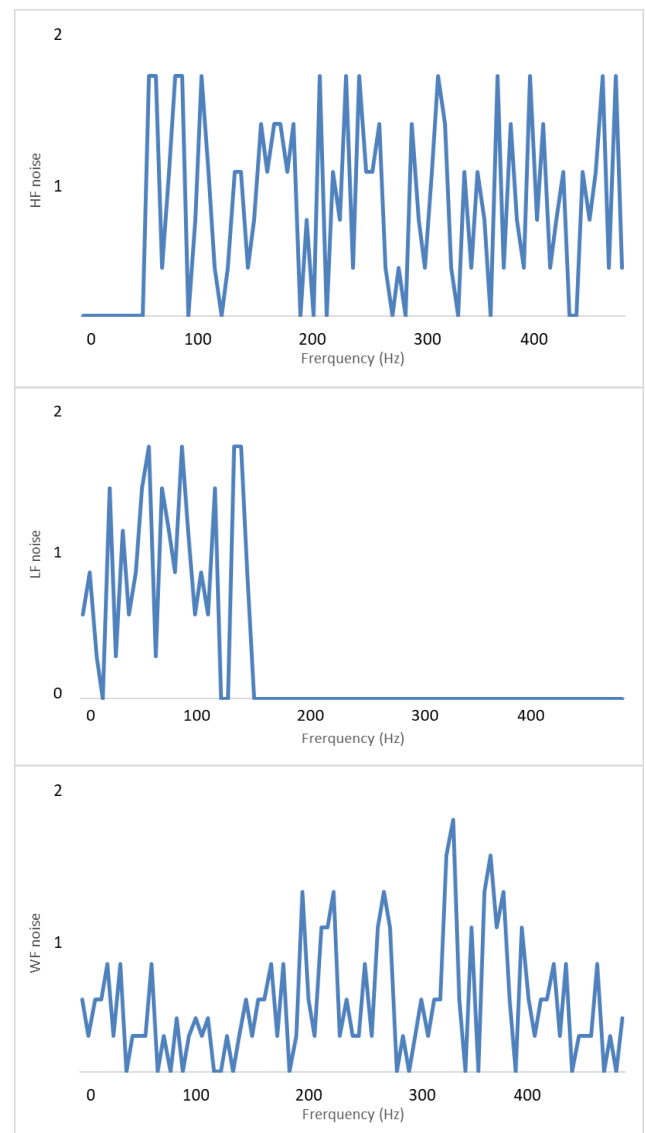


Figure 1. HF, LF, and WF noise frequency spectra

The procedures covered below are used to filter each of these distorted signals. Bland-Altman evaluation is displayed along with the coefficients associated with the original signal and SNR to a visual depiction of the accuracy of the approaches [19].

2.2 Wavelet transform

The process methods for the period-frequency area were discovered as a result of the Fourier transform's many constraints to the processing of non-stationary data. To achieve the best balance between time and frequency distinguishability, the maternal wavelet width is changed suitably in time using the WT precision [20].

2.3 Empirical Mode Decomposition

A fundamental idea behind the EMD approach was the breakdown of a complicated non-stationary signal into a group of smaller signals, or IMF. The final Residue Signal (FRS) was gathered after the repetition, the iterative EMD method calculates the maximum and minimum extremes. Every signal could be recreated using this decomposition as the residue signal plus the sum of IMFs. Due to its versatility and signal-dependency characteristics, the EMD is appropriate for the study of biomedical signals. In this investigation, a total of 10 IMFs were chosen, and the Filtered Signal (FS) is composed of the IMFs that are chosen and practically established [21].

The Chirplet Transform (CT) performs effectively for signals that resemble chirps and have linearly time-varying elements [22]. The signal transition of the S1 element to the systolic murmur and the S2 element to the diastolic murmur is not, however, depicted in the Thresholding Function (TF) plot of the diseased PCG signals [23]. The spline CT (SCT) has been derived from CT to the assessment of the TF matrix to the PCG signal. The TF localization to the non-linearly time-varying parts of the nonstationary signals is enhanced when compared with SCT with CT [24]. As a result, the pathogenic alterations can be captured more precisely and with better TF area resolution utilizing the PCG signal's TF matrix generated using SCT of the PCG signal than the one acquired via CT. The automatic evaluation of HVDs utilizing PCG signals was recently carried out using Convolutional Neural Network (CNN), Stacked Encoder (SAE) and Deep Neural Network (DNN) approaches [25]. The gradient descent method is used to implement deep learning in CNN and SAE networks to achieve the ideal parameters. Additionally, to develop these networks and achieve the ideal method variables, more examples are needed. Numerous biomedical applications also frequently use the Sparse Representation-Driven Categorization (SRC) method [26]. To forecast classification labels of evaluate characteristic vectors using these approaches, fewer attributes are needed for training cases and fewer training variables. The SRC operates better than current ML techniques for the identification of HVAs from PCG signal parameters. According to recent research, Kernel SRC (KSRC) utilizes the kernel trick to characteristic instances to greater dimensional spaces, where SRC could then be applied to categorization [27]. This enhances classification accuracy for datasets with non-linearly independent characteristic scenarios when compared to SRC alone. Therefore, the DNN created for the KSRC and ELM-auto encoder should be more efficient in the automatic identification of HVAs from the TF. It is represented by the PCG signal. SCT-based TF assessment is

employed in this study to assess the PCG recording, and non-linear properties such as permutation Entropy (PEN), Sample Entropy (SEN), and the L1-norm (LN) were calculated to the variable frequency of the PCG signal.

3. PROPOSED SYSTEM

The proposed approach of developing a hybrid Empirical Mode Decomposition (EMD) with Fast Mask Convolutional Neural Network (CNN) aims to enhance the performance measures of Phonocardiogram (PCG) signals, particularly in terms of accuracy, efficiency, and reliability in diagnosing CVD.

Empirical Mode Decomposition (EMD) is a signal processing technique used to decompose complex signals into simpler components called Intrinsic Mode Functions (IMFs), which capture different frequency components of the original signal. By decomposing PCG signals into IMFs, the hybrid EMD method aims to extract relevant features and enhance the representation of cardiac sound characteristics for more accurate analysis.

In conjunction with EMD, the integration of Fast Mask CNN introduces a deep learning-based approach to further improve the performance of PCG signal analysis. CNNs are well-suited for learning hierarchical representations of data, and the Fast Mask CNN architecture likely leverages this capability to efficiently extract discriminative features from the IMFs obtained through EMD. This hybrid approach combines the strengths of both EMD and CNNs, allowing for more robust feature extraction and classification of PCG signals. By combining EMD with Fast Mask CNN, the proposed hybrid approach offers several potential benefits. Firstly, it may enhance the accuracy of cardiac abnormality detection by effectively capturing subtle variations in PCG signals that traditional methods may overlook. Secondly, the efficiency of the Fast Mask CNN architecture likely enables faster processing of PCG signals, making the diagnostic process more time-efficient and scalable. Lastly, the reliability of the hybrid approach is expected to improve and reproducible results in CVD diagnosis, ultimately contributing to better patient outcomes and healthcare delivery.

3.1 Motivation of the work

Cardiovascular Diseases are a danger to human life in the twenty-first century and have a significant impact on socioeconomic circumstances. The method to avoid this is by early identification of cardiac problems. There are a few tests with cutting-edge technology that can evaluate the health of the heart in addition to PCG signal evaluation. However, they also take a lot of time and money. Therefore, early, low-cost, precise, and quick detection of these problems may increase the survival of persons in distress while decreasing the death rate from Cardiovascular Diseases. Cardiac auscultation, or listening to noises made by the beating of the heart, is a time-tested method for keeping track of the health of the cardiovascular system. It is a non-invasive, quick but precise, and affordable procedure that is accessible to everyone. The incorporation of cutting-edge technology in the areas of machine learning and signal processing could actively support doctors and other healthcare professionals in their attempts to improve the medical sector. The major organ of the cardiovascular system, the heart, has a great need for the

development of expert systems to monitor its health. Since diagnosing these disorders requires a high level of training and experience, the analysis of the PCG, a record of the sound the heart continuously produces, can be used to identify heart dysfunction and reduce inter-observer variability. This necessitates the purchase of HSS in digital form so that they are available for additional analysis to determine the condition of the heart. There are many different signal processing methods, but not all of them are appropriate for PCG analysis, which automatically analyses heart sounds and murmurs.

The circulatory system (CS) is in charge of transporting blood through the arteries and veins, supplying oxygen and nutrients to different organs and cells, eliminating waste products, and participating in the maintenance of a safe body temperature. In the CS, the heart was the most significant organ. It was therefore regarded as the most important organ in the human body since it constantly provides nutrition and energy to other systems, organs, or sections of the body. The heart, which is roughly the size of a fist, sits approximately in the center of the chest, behind the two lungs and just to the left of the sternum (breastbone). An envelope-like structure known as the pericardium covers it. A network of nerve tissue conducts the biopotentials that are in charge of the heart's regular rhythmic beating throughout its surface. A two-stage, four-chamber centrifugal pump could be compared to the human heart from the perspective of an engineer. The Sino Atrium (SA) Node, a collection of cells also referred to as pacemaker cells, produces biopotentials that the heart uses to pump blood. The ECG reflects the rhythmic activity of the heart and is a record of such bio potentials when they are set up properly. The heart is a muscular organ that has four chambers: the Left Atrium (LA), Right Atrium (RA), Right Ventricle (RV), and Left Ventricle (LV). The heart is divided into two phases, the Atrium and the Ventricle. Its duties are to provide the entire body with energy, including all of the functional organs, produce oxygenated blood to serve as the energy carrier, and transport deoxygenated blood to the lungs where it is oxygenated and carbon dioxide is expelled. In particular, it draws polluted blood from the body through the LA and RA, purifies it in the lungs, and distributes the clean blood to the various organs of the body, including the heart, through the LV and RV. The muscles of the ventricles are stronger than those of the atrium because they are responsible for distributing blood throughout the body. To transport blood into and out of the heart, veins, and arteries are joined to the heart. Veins carry impure or deoxygenated blood, whereas arteries carry pure or oxygenated blood. To regulate the flow of blood between the different heart chambers, valve configurations are in place. The left and right atria's two chambers are divided by the mitral and tricuspid valves, respectively. However, the aortic and pulmonary valves separate the left and right ventricles, the two chambers of the ventricle. A fibrous cardiac skeleton supports the four heart valves. The ventricular and atrial muscles, and the valves, are attached to this skeleton, which is formed of dense connective tissue. The heart wall is made up of three stages: the innermost part is thin and is known as the endocardium, the middle layer is somewhat thick and is characterized as the myocardium, and the outermost part is thin and is characterized as the epicardium. Many blood arteries link to the heart and fall into the following categories: The arteries deliver pure (oxygenated) blood to various organs and body parts, whereas the veins collect impure (deoxygenated) blood from various body parts and organs.

3.2 Proposed method

The method of denoising extracts the information from the noisy signal by separating it from the noise. The remaining portion that is regarded as noise would be removed, resulting in the creation of a new signal to the necessary characteristics (like S2 and S1 to PCG) in terms of the frequency data. The signal and noise were separated using the denoising approach, as opposed to a filter based on certain frequencies that will be kept or eliminated. A collection of thirty *.wav heart sounds, with a total duration of 33, 37 ± 5,81s and 23 normal and seven aberrant heart sounds, was used. The subjects' age and gender have not been disclosed. Every recording has been sampled using a 2000 Hz frequency.

3.2.1 Data acquisition process

Describe the source of the Phonocardiogram (PCG) signals, whether they were obtained from clinical recordings, publicly available datasets, or generated synthetically.

Specify the hardware used for data acquisition, such as PCG sensors, amplifiers, and data acquisition systems.

Detail the recording protocol, including patient positioning, sensor placement on the chest, and any relevant environmental conditions during data collection.

Provide information on the demographic characteristics of the study population, including age, gender, and any relevant clinical conditions.

3.2.2 Pre-processing steps

Outline the pre-processing steps applied to the raw PCG signals to enhance their quality and facilitate subsequent analysis.

Include procedures for signal filtering to remove noise and artifacts, such as baseline drift and high-frequency noise.

Describe any signal normalization techniques employed to ensure consistency across recordings and mitigate amplitude variations.

Detail any artifact removal methods used to eliminate non-cardiac sounds and motion artifacts from the PCG signals.

Specify the sampling rate and any downsampling or resampling procedures applied to the PCG signals.

3.2.3 Implementation details of EMD-FMCNN approach

Provide a step-by-step description of the implementation of the hybrid EMD-FMCNN approach for PCG signal analysis.

Explain the process of decomposing the pre-processed PCG signals into Intrinsic Mode Functions (IMFs) using Empirical Mode Decomposition (EMD), including any parameter settings or variations used.

Detail the architecture of the Fast Mask Convolutional Neural Network (CNN) utilized for feature extraction and classification of the IMFs.

Specify the hyperparameters of the CNN, including the number of layers, filter sizes, activation functions, and optimization algorithms.

Describe the training process of the CNN, including the dataset used for training, data augmentation techniques applied, and evaluation metrics used to assess model performance.

Outline any post-processing steps applied to the CNN outputs, such as thresholding or ensemble methods, to improve classification accuracy.

EMD-FMCNN and a different thresholding technique were used in this study to carry out the denoising process. The

system efficiency of the denoising approach was determined by SNR and MSE for both EMD-FMCNN and DD-DWT. The investigation was restricted to signals that were AWGN-corrupted and had all frequencies with similar amplitudes, indicating that the power density was frequency-dependent. If a measured signal $a(t)$ contains white Gaussian noise $N(0,1)$,

$$a(t)=f(t)+\sigma n(t) \tag{1}$$

$f(t)$ is the original signal, $n(t)$ is the noise, and σ is the noise strength (standard deviation). In this investigation, SNR 10 dB and $r = 1$ were utilized. σ - noise strength; $f(t)$ - original signal and $n(t)$ is the noise. The goal of the denoising procedure is to remove the signal's sound to recover $f(t)$. The process employed in this work is shown in Figure 2. The loading of the PCG dataset was the first phase in this work's PCG signal extraction method followed by a normalized and centered preprocessing step. The PCG signal was denoised using either the DD-DWT or the EMD-FMCNN in the following stage. The final phase in our study of describing the system's efficiency was to determine the SNR and MSE value after the denoising procedure. To analyze the PCG non-stationary signals, the EMD-FMCNN and DD-DWT technology breaks the signal down into a collection of fundamental signals. The PCG signal was denoised using either the DD-DWT or the EMD-FMCNN in the following stage.

The PCG signal $a(t)$ is broken down by the EMD-FMCNN into many IMF. The time gap between the two extrema could be used to accurately characterize the IMF based on its time-scale properties [11]. The greatest frequency oscillation left in the signal is chosen by the EMD-FMCNN. As a result, every IMF has an oscillation with an LF than the one that was previously obtained locally. Additionally, The EMD-FMCNN used either a wavelet or filter operation that has been predetermined. EMD-FMCNN decomposition works for both nonlinear and non-stationary activities since it is the local features and time scale of the information. The EMD breaks down into a collection of IMFs that must meet two requirements: (1) It should be symmetric to the local mean and (2) It must have a different number of zero crossings and extrema. The following stages are some of the procedures used by the EMD technique to deconstruct $a(t)$ to a sum of the IMFs:

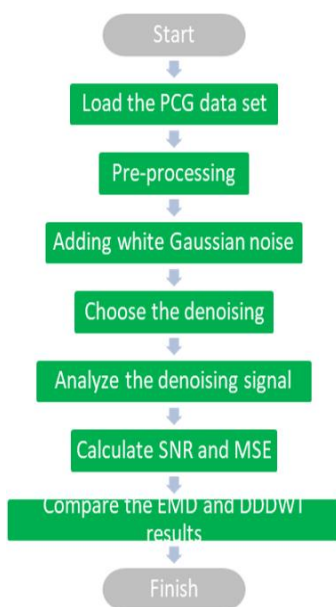


Figure 2. The workflow process

1. To obtain the upper and lower envelopes and to find local maximum and minimum values in $a(t)$ using SCT.

2. To determine $m(t)$ (average mean) by combining the upper and lower envelopes.

3. To determine $h(t)$ (the temporary local oscillation) by subtracting $a(t)$ with $m(t)$.

$$h(t) = a(t) - m(t)$$

4. To determine $h(t)$'s median; if it is near zero then $h(t)$ is the first IMF called $c_x(t)$ else repeat steps (1) - (3) by substituting $h(t)$ for $x(t)$.

$$\text{To calculate } r(t) \text{ (remainder)} = a(t) - c_x(t)$$

5. To get the subsequent IMF and residue, repeat steps 1 through 5 using $r(t)$ instead of $a(t)$.

6. Decomposition comes to an end when $r(t)$ turns into a constant that no longer meets the requirements.

$$a(t) = \sum_{x=1}^N c_x(t) + r(t) \tag{2}$$

Thresholding and statistics categorization are required for the IMF-based denoising approach employing EMD. Conditions must be fulfilled by the IMF, a group of activities.

The highest and lowest sums (total of extrema) must not exceed one or be equal to the entire amount of zero-crosses. The other version of DWT, such as DD-DWT, could be employed to evaluate heart sounds because (DWT) methods are widely utilized for this purpose. The procedure for denoising using DD-DWT is shown in Figure 3.

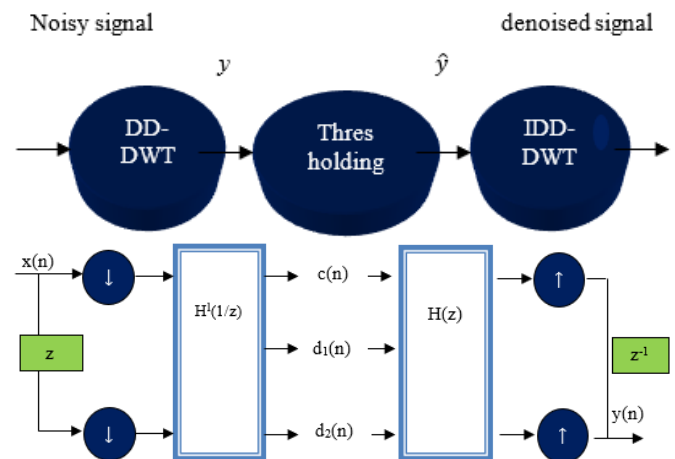


Figure 3. The design of the DD-DWT method employed with TF to denoising and its filter

Thresholding is one of the most effective signal-denoising methods, reducing the likelihood of high-frequency signal and noise mingling. Hard thresholding and soft thresholding are the 2 kinds of criteria that are utilized in this research. The features of the two thresholding methods employed in this investigation are shown in Figure 4. ρ is a thresholding value and $a_y(k)$ is a decomposition signal. Eq. (3) describes the hard-thresholding procedure.

$$\hat{t}_y = \begin{cases} a_y(k), & |a_y(k)| > \rho \\ 0, & |a_y(k)| \leq \rho \end{cases} \tag{3}$$

The method of soft-thresholding described in Eqs. (4) and (5).

$$\text{sign}a_y = \begin{cases} 1, a_y(k) > 0 \\ 0, a_y(k) = 0 \\ -1, a_y(k) < 0 \end{cases} \quad (4)$$

$$\bar{t}_y(k) = \text{sign}[a_y(k)] \times |a_y(k) - \rho_y| \quad (5)$$

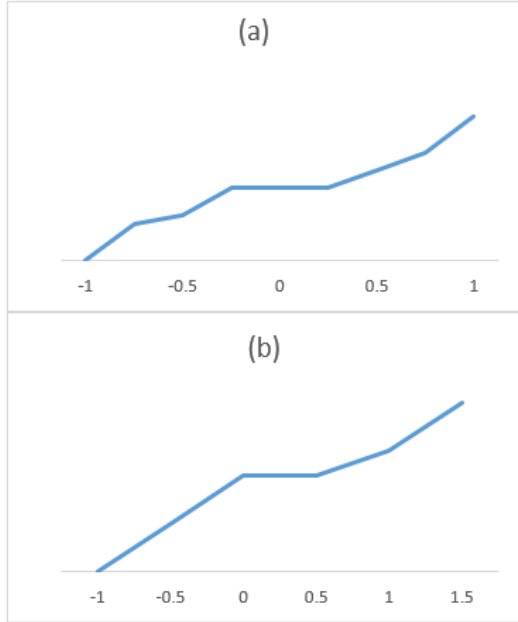


Figure 4. Evaluation of the TF (a) hard thresholding and (b) soft thresholding

The EMD-FMCNN is proposed in this article as a method for automatically classifying HVDs using the properties of retrieved PCG signals. Figure 5 illustrates the EMD-FMCNN's architectural layout. Using 10-fold CV and hold-out approaches, the training and test PCG records are chosen. Figure 6 determines the flow chart of the proposed techniques to automatically identify and categorize HVDC into normal and pathological (Aortic Stenosis (AS), Mitral Regurgitation (MR), Mitral Valve Prolapse (MVP) and Mitral Stenosis (MS)) states using EMD-FMCNN. The following subsections provide a detailed explanation of each of the steps in the proposed method.

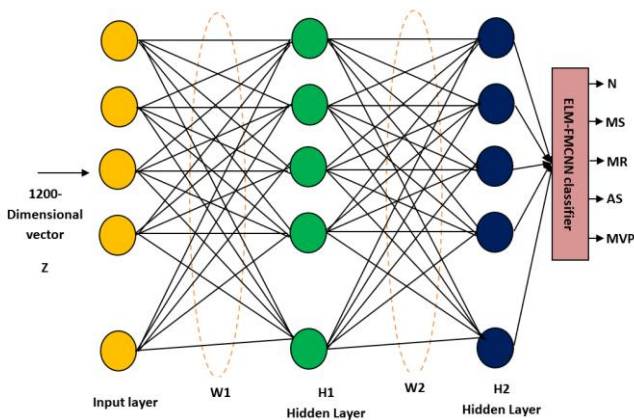


Figure 5. The proposed EMD-FMCNN framework for classifying HVDs

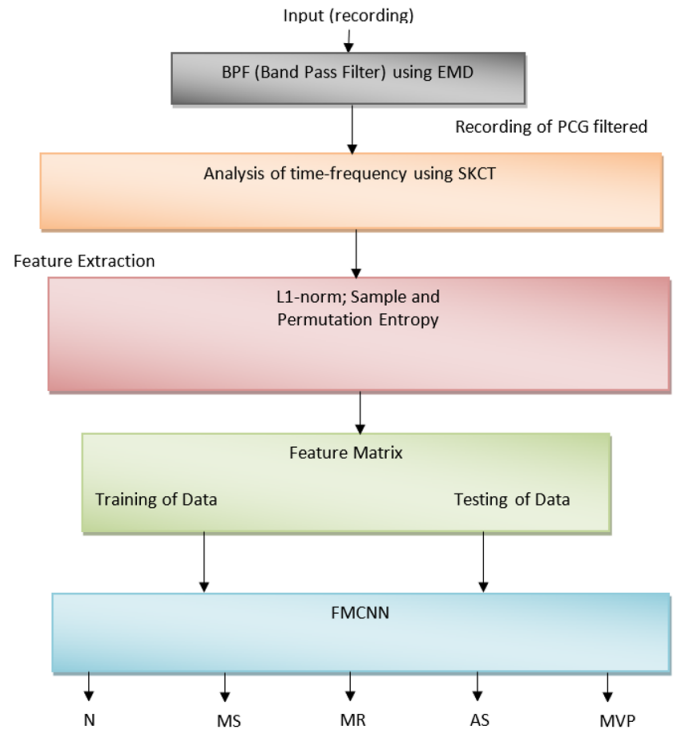


Figure 6. The recommended approach for automated HVD identification and categorization

Collected and Filtered PCG Signals are utilized in our research, we employed PCG recordings from a public database 1 is described in depth. One thousand PCG recordings from various groups are included in the dataset. Of the 1000 recordings, 200 PCG recordings are found in each of the two classes (normal and diseased). The dataset includes the annotations for the pathological (MS, AS, MVP, and MR) and normal (N) categories of PCG signals. Each PCG recording features a 16-bit resolution and an 8-kHz sampling rate. The gathered PCG recordings in this study are down-sampled to 4 kHz for the TF evaluation. PCG signals of the EMD-FMCNN were also utilized. It comprises both normal and pathological (44.1 kHz sampling frequency) PCG signals (AS, MS, MR, and MVP). Additionally, these signals are down-sampled to 4 kHz. The researcher also employed real-time PCG signals captured for this research. The subjects have given written agreement to the non-invasive recording of the PCG signal. Each recorded signal has a sample frequency of 4 kHz. The noise that characterizes PCG signals is removed using a 6th-order Butterworth BPF having 25 Hz and 900 Hz lower and higher cutoff frequencies. Following filtering, the PCG recording's greatest amplitude value is used to conduct amplitude normalization. Each PCG recording's TF representation is calculated utilizing SCT following normalization. The subsection that follows provides a description of the spline kernel-based CT for evaluating the TF matrix obtained from PCG recording.

The CT to a changed kernel operation is the SK and CT. TF representation to the non-stationary signal is implemented using many frequency rotation and frequency shift operators in this modified kernel function. Following is an evaluation of the separate SCT for a PCG signal with N samples, $a[n]$:

$$T[\tilde{n}, k] = \sum_{n=0}^{N-1} \tilde{t}[n] w_{\sigma}[n - \tilde{n}] e^{-y \frac{2\pi n k}{N}} \text{ for } \tilde{n} \in [n_x, n_{x+1}] \quad (6)$$

With $\tilde{i}[n] = i[n] \cdot \varphi^R[n, Q] \cdot \varphi^S[n, \tilde{n}, Q]$. T stands for the TF matrix, where the frequency-rotate and frequency-shift functions are $\varphi^R[n, Q]$ and $\varphi^S[n, \tilde{n}, Q]$, correspondingly.

$$w_\sigma[n] = \frac{1}{\sqrt{2\pi\sigma}} e^{-\frac{n^2}{2\sigma^2}} \quad (7)$$

As seen in Eqs. (8) and (9) respectively, are the frequency-rotate generator and frequency-shift operator, respectively.

$$\varphi^R[n, Q] = e^{(-\gamma \sum_{l=1}^L q_l^x [n-n_x]^l + \gamma x)} \quad (8)$$

$$\varphi^S[n, \tilde{n}, Q] = e^{(\gamma \sum_{l=1}^L q_l^x [\tilde{n}-n_x]^l - 1)n} \quad (9)$$

where, $Q[i, l] = q_l^x$ denotes SK-CT. The variable γ_x in SCT should meet the requirements listed in Eq. (10).

$$\gamma_x - \gamma_{x+1} = \sum_{l=1}^L \frac{q_l^{x+1}}{l} [n_x - n_{x+1}]^l \quad (10)$$

$$\text{MSE} = \frac{1}{n} \sum_{i=1}^n (Y_i - \hat{Y}_i)^2 \quad (11)$$

$$\text{SNR} = \frac{P_{\text{signal}}}{P_{\text{noise}}} \quad (12)$$

4. RESULTS AND DISCUSSIONS

This study employed thirty PCG signals in *.wav format from Computing in Cardiology Physionet analyze the system performance. They only utilized the single input shown in Figure 7 to analyze the denoising procedure. In this analysis, the signal length is one second and fifteen seconds. S1 and S2 are sequenced in the input signal depicted in Figure 8. The signal used in this image is a PCG from a healthy heart state, as seen by this image. The denoised PCG signal outcome is produced by EMD-FMCNN which is depicted in Figure 9. The DD-DWT approach may eliminate the sound artifact to the PCG signal based on the results. The PCG signal is divided into many IMF signals by the EMD-FMCNN deployment. To obtain denoised PCG for this work, we employed the fourth layer decomposition. Figure 10 compares the SNR values for the denoising using EMD-FMCNN and DD-DWT.

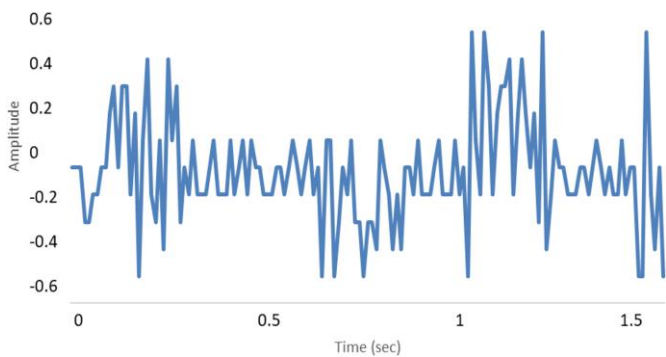


Figure 7. Analyze the denoising procedure of PCG

When using a soft thresholding technique, SNR values are distributed more evenly than when using a hard thresholding

method. Additionally, compared to the DD-DWT approach, the EMD-FMCNN technique of denoising PCG signal methods exhibits a greater SNR value.

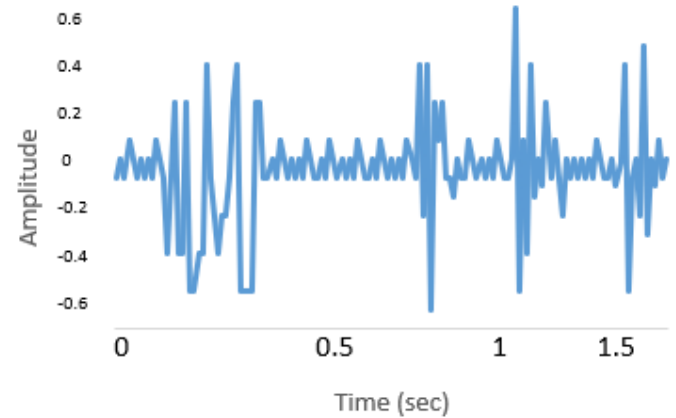


Figure 8. Compares the S1 and S2 signal of SNR values

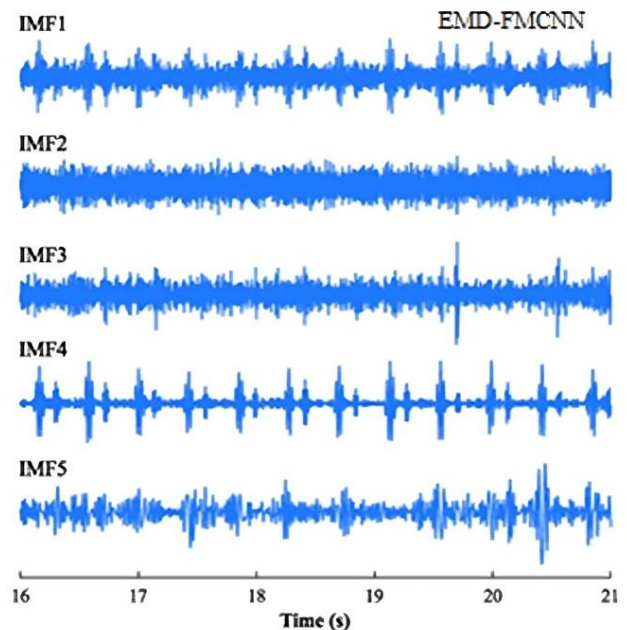


Figure 9. The EMD-FMCNN method to obtain the denoised PCG signal

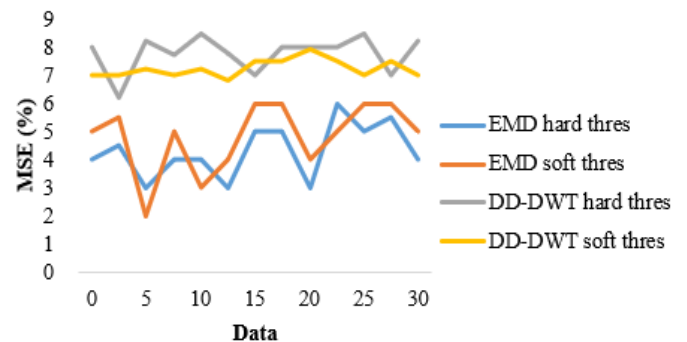


Figure 10. Compare the SNR values for the denoising using EMD-FMCNN and DD-DWT

In Figure 11, the MSE values of the two employed approaches are compared. When using the soft thresholding

method, MSE values are distributed more evenly than when using the hard thresholding method. Additionally, the MSE value for PCG signal-denoising systems using the EMD-FMCNN approach is lower than for systems using the DD-DWT method. The greatest MSE values for the soft threshold-based DD-DWT system and the soft threshold-based EMD-FMCNN system are 0.14695 and 0.00344, respectively. EMD-FMCNN outperformed the DD-DWT method using the MSE score as a benchmark. In the statistical study, the SNR score for EMD-FMCNN with a hard criterion is 16.75 ± 2.17 dB, and for EMD-FMCNN with a soft threshold is 21.99 ± 2.1 dB. The denoising system's outcomes for the EMD-FMCNN hard and soft thresholds, based on MSE value, were 0.01 ± 0.005 and 0.01 ± 0.007 , respectively. For hard and soft thresholds, accordingly, the MSE value for DD-DWT is 1.13 ± 0.25 and 0.42 ± 0.12 . When comparing average values, EMD surpasses DD-DWT in terms of SNR and MSE. We utilized an ANOVA to evaluate the comparability of outcomes between the EMD-FMCNN and DD-DWT. BPF comparison among the DD-DWT and EMD-FMCNN soft thresholds is shown in Figure 12.

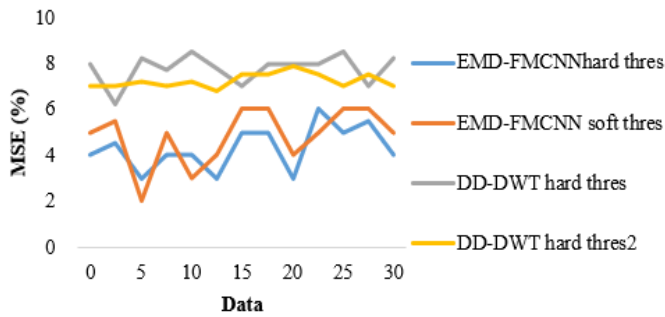


Figure 11. Compare the MSE values for the denoising using EMD-FMCNN and DD-DWT

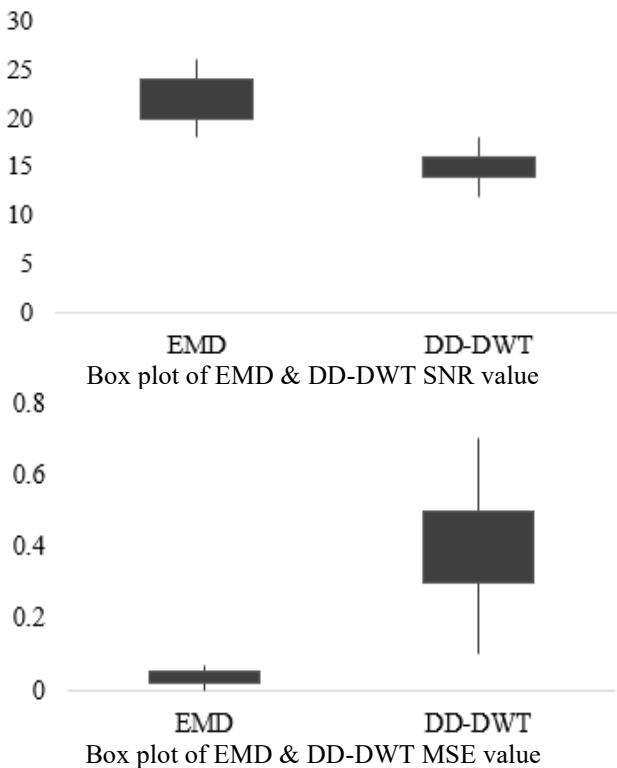


Figure 12. Compare the boxplot of MSE and SNR values for the denoising using EMD-FMCNN and DD-DWT

It obtained the p-values of MSE and SNR based on an ANOVA 9.43×10^{-23} and 3.05×10^{-26} respectively. According to ANOVA, the tiny p-values for MSE and SNR show that there are substantial variations among the DD-DWT and EMD-FMCNN. Therefore, the scope of this investigation was restricted to signals tainted with AWGN, the findings support the assertion made that EMD-FMCNN outperforms DD-DWT in terms of performance. According to the study, EMD-FMCNN performs better than the Wavelet Transform (WT) and Total Variation (TV) methods shown in Figure 13 (a-c).

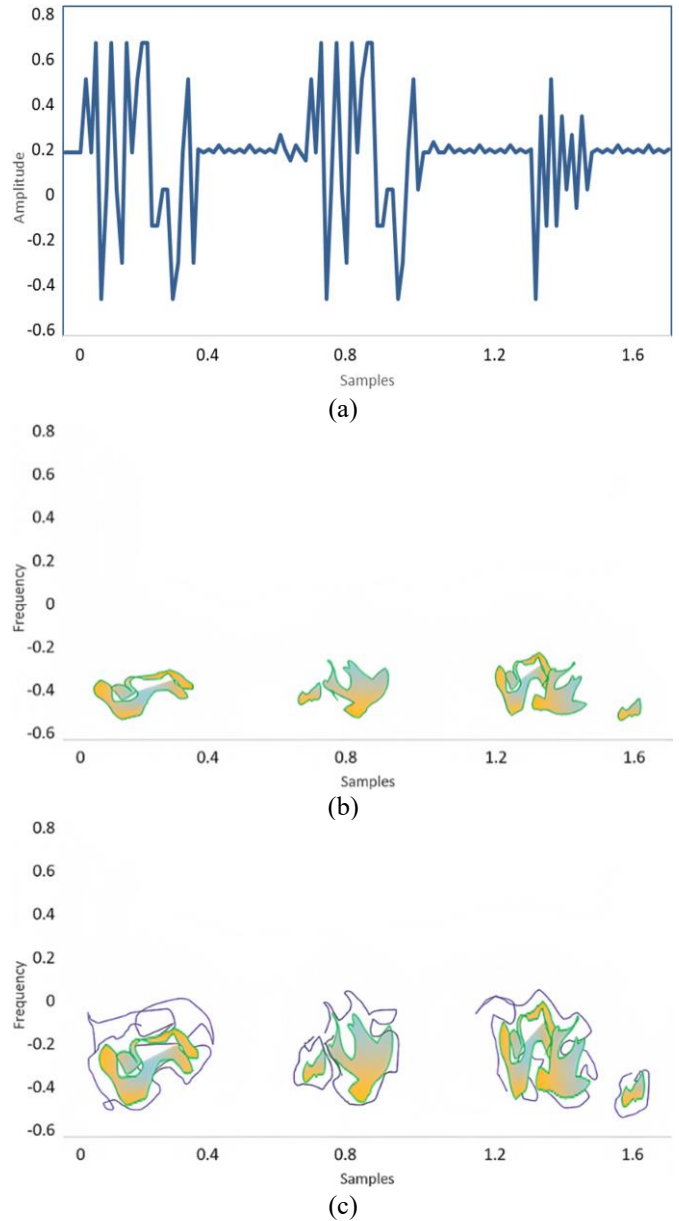
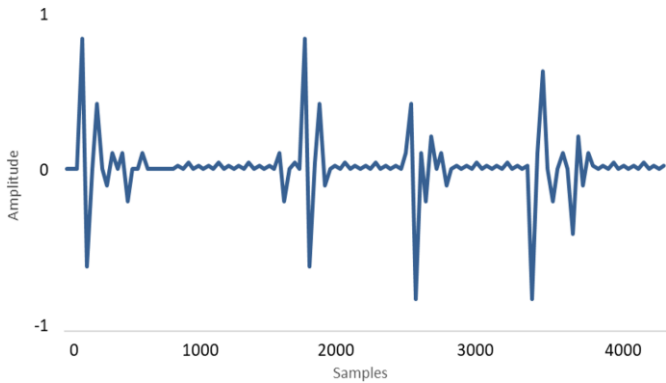


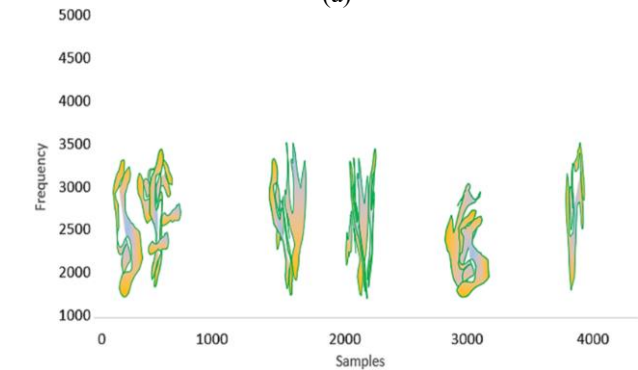
Figure 13. (a) AS present in Pathological PCG signal between the S1 and S2 (each cardiac cycle's) components. (b) Depicted abnormal PCG signals (Time Frequency) using CT. (c) Depicted abnormal PCG signals (Time Frequency) using SK-CT

Figures 14 (a, c, e, g, i) correspondingly show the PCG signals of (N) and pathological categories to MVP, MVP, MR, and MS. Figures 14 (b, d, f, h, j) respectively show the corresponding TF plots for these signals gathered through SCT. When compared to a normal PCG signal, it could be seen that the variation connected to a pathological PCG signal was a varied morphology depending on the kind of HVD. The

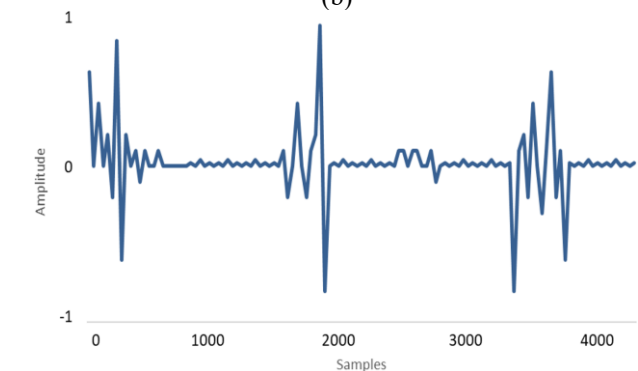
energy of the S2 and S1 elements of the typical PCG signals were broadly dispersed between 25 Hz and 300 Hz (as illustrated in Figure 14 (b)). Therefore, in HVD situations, the power was dispersed over 300 Hz and is seen in those PCG signal's TF graphs. Regarding both normal and abnormal PCG signals, every frequency element in the TF matrix of the PCG recording has a separate set of properties. The traits that may be determined using them are thus useful for the precise detection of HVDs. The assessment of the L1-norm (LN) properties for the k th frequency element is shown in Table 1.



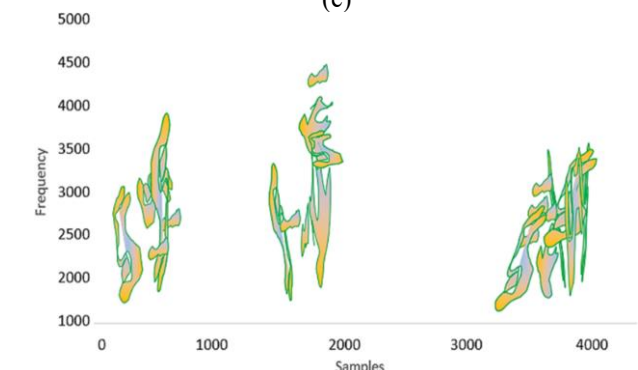
(a)



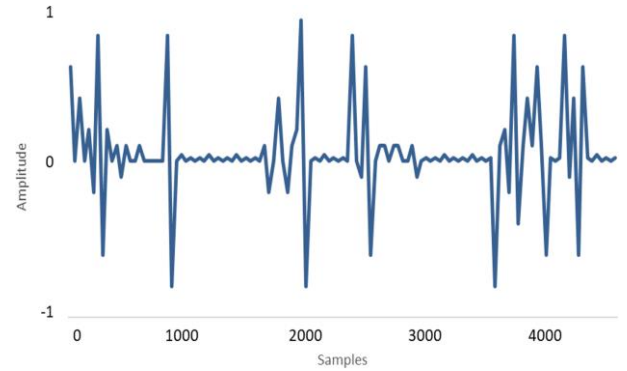
(b)



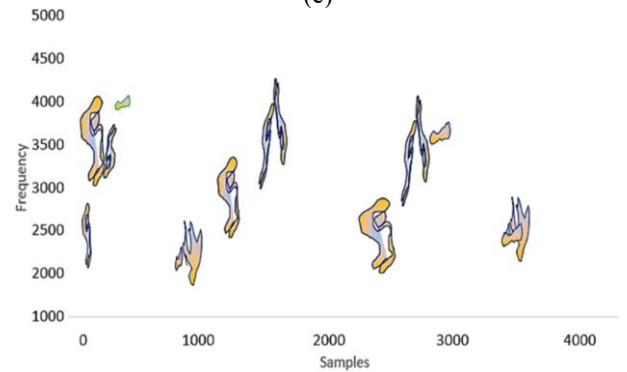
(c)



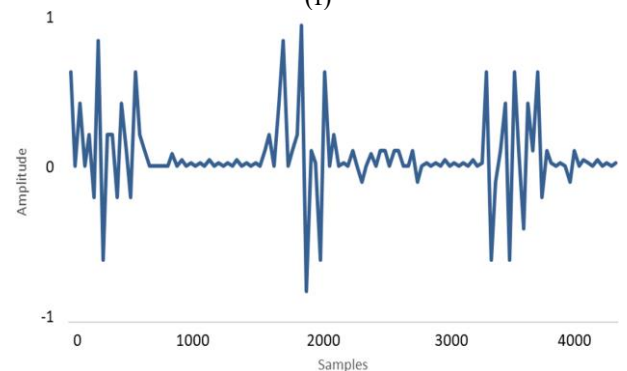
(d)



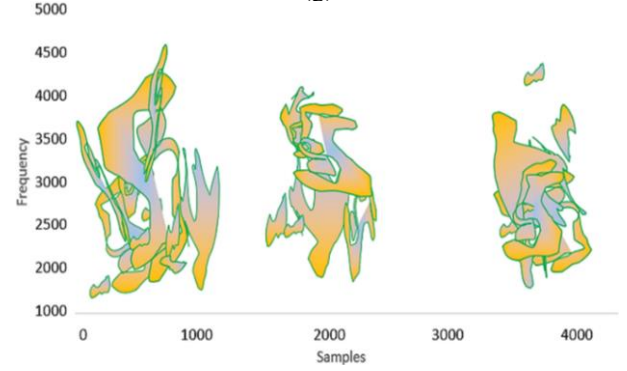
(e)



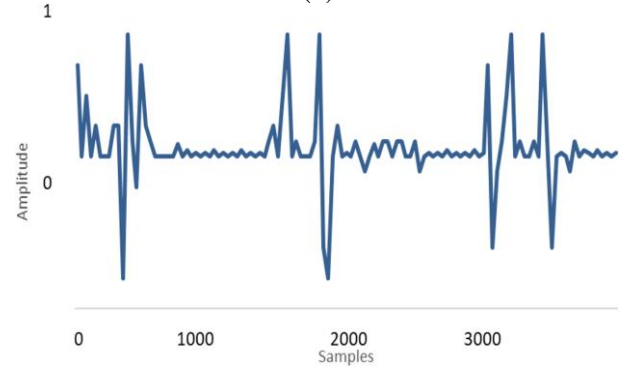
(f)



(g)



(h)



(i)

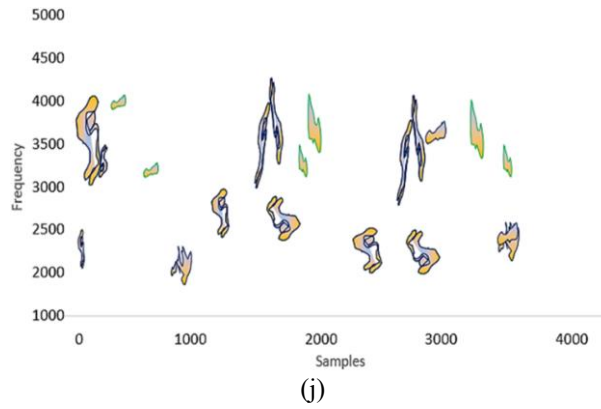


Figure 14. (a) An example of an ordinary class PCG record. (b) A normal PCG signal represented time frequency that was acquired via SCT. (c) MR class PCG record. (d) A depiction of the MR PCG signal's time and frequency produced by SCT. (e) MS category PCG record. (f) A depiction of the MS PCG signal's time and frequency obtained by SCT. (g) AS category PCG record. (h) An AS PCG signal acquired using SCT is represented in time and frequency. (i) MVP category PCG record. (j) A depiction of the MVP PCG signal's duration and frequency received by SCT

Table 1. The classification outcomes for the automated identification of HVDs using EMD-FMCNN algorithms using SCT area characteristics

Classifier	Class	Performance Measure								OA (%)
		TP	TN	FP	FN	Sensitivity %	Precision %	F-Score %	Specificity %	
RF	N	61	228	0	0	97.80 ± 2.65	98.35 ± 2.37	99.41 ± 0.75	98.10 ± 1.52	96.62
	MS	61	228	7	0	88.71 ± 3.78	96.88 ± 1.40	96.75 ± 1.32	92.58 ± 1.92	
	MR	50	239	2	1	96.32 ± 1.88	87.98 ± 4.66	99.15 ± 0.43	91.45 ± 3.22	
	AS	60	229	2	2	96.62 ± 3.40	95.38 ± 1.83	97.92 ± 1.06	93.80 ± 1.65	
	MVP	606	229	6	2	98.35 ± 1.25	93.35 ± 4.58	99.65 ± 0.32	95.69 ± 2.82	
KNN	N	58	232	0	1	98.72 ± 1.36	99.69 ± 0.75	99.66 ± 0.38	99.18 ± 0.83	98.00
	MS	60	235	4	0	90.18 ± 1.66	97.68 ± 0.92	97.29 ± 0.50	93.77 ± 1.29	
	MR	59	233	3	2	97.95 ± 1.51	94.01 ± 3.47	99.54 ± 0.37	95.91 ± 2.20	
	AS	58	234	4	3	98.25 ± 2.12	92.02 ± 3.22	99.66 ± 0.53	95.01 ± 2.21	
	MVP	61	235	2	4	96.44 ± 2.57	97.35 ± 1.92	99.08 ± 0.72	96.86 ± 1.77	
KSRC	N	60	237	0	0	100.0 ± 0.00	100.0 ± 0.00	100.0 ± 0.00	100.0 ± 0.00	99.51
	MS	61	238	1	2	96.14 ± 2.14	98.98 ± 0.92	98.99 ± 0.57	97.55 ± 1.53	
	MR	59	237	0	3	98.68 ± 2.18	97.68 ± 1.92	96.97 ± 0.55	98.16 ± 1.90	
	AS	60	239	0	0	99.01 ± 1.50	96.99 ± 1.19	99.16 ± 0.52	97.97 ± 1.30	
	MVP	61	238	4	1	96.72 ± 1.19	99.16 ± 0.55	99.67 ± 0.18	96.68 ± 1.03	
EMD-FMCNN	N	60	239	0	2	100.0 ± 0.00	100.0 ± 0.00	100.0 ± 0.00	100.0 ± 0.00	99.83
	MS	61	240	2	0	98.24 ± 1.04	99.03 ± 0.12	99.00 ± 0.65	99.15 ± 0.18	
	MR	61	239	2	2	99.04 ± 0.25	98.79 ± 1.30	98.89 ± 0.17	99.00 ± 0.28	
	AS	59	239	0	2	99.20 ± 0.65	97.96 ± 1.39	99.83 ± 0.02	98.73 ± 1.35	
	MVP	60	240	2	3	96.90 ± 1.04	97.37 ± 1.30	99.57 ± 0.13	97.52 ± 1.85	

Table 2. The classification outcomes for automated PCG diagnosis utilizing many classifiers with the SCT area

Method	Class	Sensitivity %	Precision %	F-Score %	Specificity %
EMD-FMCNN	N	98.11 ± 2.08	100 ± 0.00	99.52 ± 0.57	99.02 ± 1.08
	MS	93.88 ± 2.99	96.01 ± 0.91	98.40 ± 0.82	94.92 ± 1.75
	MR	96.44 ± 2.36	96.68 ± 2.37	99.05 ± 0.65	96.52 ± 0.70
	AS	98.32 ± 1.69	94.35 ± 1.92	99.60 ± 0.45	96.27 ± 0.78
	MVP	97.25 ± 2.31	96.35 ± 2.19	99.25 ± 0.57	96.65 ± 1.28

Table 1 reveals that the EMD-FMCNN classification's OA value was great that there are 800 and 600 neurons in the 1st and 2nd hidden levels, correspondingly. By adding more neurons to both hidden layers, the OA value falls. The classification outcomes achieved using the EMD-FMCNN classifier for the PCG signals acquired from the MHSMD database are provided in Table 2. EMD-FMCNN algorithms using SCT Area characteristics is shown in Figure 15.

It is necessary to choose the IMFs that can be retained for signal structure and that would be discarded when utilizing EMD-FMCNN to filter signals. Ten IMFs are calculated across every instance of the study; however, various IMFs and

various numbers are selected for the signal construction to get the best results feasible. In general, the 6th, 5th, and 4th, IMFs are chosen to remove HF and WF noise, which included the 7th IMF, except for the pat2 signal. Furthermore, the IMFs chosen for each signal, and the instance of the LF noise were different (for phy2's third and fourth IMF and pat1 and pat2's second and third IMF phy1's third, fourth, and fifth IMF). The results of EMD-FMCNN filtering are shown in Table 3 of fall scenarios. The EMD-FMCNN technique scores worse than WT filtration, filtering HF, and WF noise, in terms of association and SNR enhancement. Nonetheless, SNR values increased in comparison to WT, when applied to LF noise,

reaching positive levels; nonetheless, the correlation was much smaller. It should be observed that the SNR values and correlation for the pat1 signal, which presented challenges for WT filtering, are equivalent to those for findings from other signals. As a consequence, the EMD-FMCNN approach is more effective when high-frequency elements like murmurs are present in the signal as shown in Table 4.

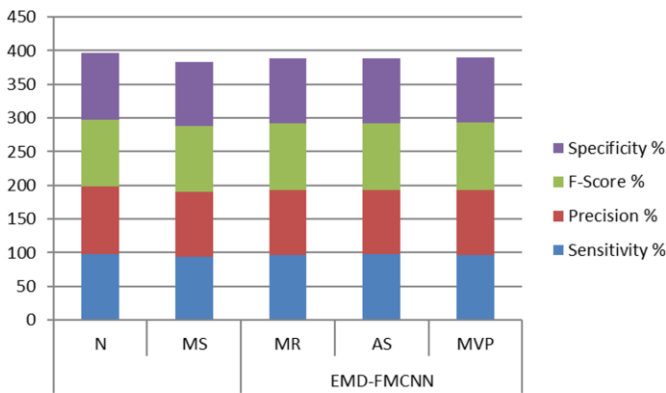


Figure 15. EMD-FMCNN algorithms using SCT Area characteristics

Table 3. Results of EMD-FMCNN

Signals Type	SNR (dB)			Coefficient of Correlation		
	HF	LF	WF	HF	LF	WF
phy1	3.394	1.995	3.6988	0.4911	0.5961	0.4869
phy2	6.218	2.089	4.5022	0.7634	0.5198	0.6516
pat1	4.842	1.774	5.3047	0.6693	0.4619	0.6488
pat2	5.582	2.614	5.6747	0.7432	0.6047	0.7229

Table 4. Overall performance measures of EMD-FMCNN

ACC (%)	SE (%)	PPV (%)	F1 (%)
94.99±0.70	97.41±0.51	97.44±0.49	97.46±0.37

5. CONCLUSIONS

Researchers examine the DD-DWT and EMD-FMCNN methods as denoising systems to reduce the sound impact of the PCG signal to find an effective way for the PCG system. The SNR and MSE parameters were used to evaluate different denoising techniques for signal noise suppression. According to the findings, the EMD-FMCNN denoising approach outperformed the DD-DWT in terms of MSE and SNR. According to ANOVA, the tiny p-values of MSE and SNR show that there are significant variations between EMD-FMCNN and DD-DWT. Researchers made the case that the EMD-FMCNN approach is preferable for eliminating noise from PCG signals. Researchers working on an automated system for the localization and categorization of heart sounds will find these results to be of great value as well. This paper suggests an automatic HVD detection and categorization of PCG signals. This method computed the TF representation of PCG records using SCT. The frequency elements of the TF representation are used to calculate the nonlinear characteristics (LN, PEN, and SEN). The FMCNN classification dynamically divides PCG signals into four HVD category categories using the collected characteristics. The effectiveness of the recommended method was also determined using the real-time record PCG signals, and the

results gained demonstrate this. In the future, researchers intend to improve this method to use PCG signals to detect coronary artery disease and stress.

REFERENCES

- [1] González-Rodríguez, C., Alonso-Arévalo, M.A., García-Canseco, E. (2023). Robust denoising of phonocardiogram signals using time-frequency analysis and U-Nets. *IEEE Access*, 11: 52466-52479. <https://doi.org/10.1109/ACCESS.2023.3280453>
- [2] Reddy, N.S.S., Reddy, V.P.M.S., Mohan, N., Kumar, S., Soman, K.P. (2023). A fast iterative filtering method for efficient denoising of phonocardiogram signals. In 2023 3rd International Conference on Intelligent Technologies (CONIT), Hubli, India, pp. 1-6. <https://doi.org/10.1109/CONIT59222.2023.10205633>
- [3] Hasan, A., Bahri, Z. (2023). Comparative study on heart anomalies early detection using phonocardiography (PCG) signals. *International Journal of Computing and Digital Systems*, 14(1): 1023-1040. <https://doi.org/10.12785/ijcds/140180>
- [4] Ali, S.N., Shuvo, S.B., Al-Manzo, M.I.S., Hasan, A., Hasan, T. (2023). An end-to-end deep learning framework for real-time denoising of heart sounds for cardiac disease detection in unseen noise. *IEEE Access*, 11: 87887-87901. <https://doi.org/10.1109/ACCESS.2023.3292551>
- [5] Das, P., Ray, A. (2023). Hardware-efficient FIR filter design using fast converging flower pollination algorithm—A case study of denoising PCG signal. In *Hybrid Computational Intelligent Systems*, pp. 263-278.
- [6] Shervegar, V.M. (2023). A robust sliding window adaptive filtering technique for phonocardiogram signal denoising. *Expert Systems*. <https://doi.org/10.1111/exsy.13361>
- [7] Satyasai, B., Sharma, R., Bansal, M. (2023). A gammatonegram based abnormality detection in PCG signals using CNN. In 2023 3rd International Conference on Artificial Intelligence and Signal Processing (AISP), Vijayawada, India, pp. 1-5. <https://doi.org/10.1109/AISP57993.2023.10134986>
- [8] Wang, J., Zang, J., An, Q., Wang, H., Zhang, Z. (2023). A pooling convolution model for multi-classification of ECG and PCG signals. *Computer Methods in Biomechanics and Biomedical Engineering*. <https://doi.org/10.1080/10255842.2023.2299697>
- [9] Lubaib, P., Beegum, D., Muhsina, N., Manjusree, S., Al Saheer, S.S. (2023). Development of an efficient cardiac auscultation system using proper denoising techniques. In 2023 Third International Conference on Advances in Electrical, Computing, Communication and Sustainable Technologies (ICAECT), Bhilai, India, pp. 1-8. <https://doi.org/10.1109/ICAECT57570.2023.10118133>
- [10] Talal, M., Aziz, S., Khan, M.U., Ghadi, Y., Naqvi, S.Z.H., Faraz, M. (2023). Machine learning-based classification of multiple heart disorders from PCG signals. *Expert Systems*, 40(10): e13411. <https://doi.org/10.1111/exsy.13411>
- [11] Jatia, N., Veer, K. (2023). Performance comparison of denoising methods for fetal phonocardiography using fir filter and empirical mode decomposition (EMD). In *Optimization Methods for Engineering Problems*, pp.

- 171-183.
- [12] Akermi, R., Younes, R.B., Saadaoui, W. (2023). An intelligent medical platform for PCG signal preprocessing for patients with mechanical double-winged prostheses valve. *International Journal of New Technology and Research*, 9(5): 1-6. <https://doi.org/10.31871/IJNTR.9.5.10>
- [13] Hakkoum, K., Cherif, L.H. (2023). Accurate segmentation of phonocardiogram signals using fractal decomposition with WB-MFA in MATLAB 2022. In *International Conference on Pioneer and Innovative Studies*, Konya, Turkey, pp. 25-27. <https://doi.org/10.59287/icpis.800>
- [14] Gadde, Y., Kumar, T.K. (2023). Prediction of heart abnormality using heart sound signals. In *Machine Intelligence Techniques for Data Analysis and Signal Processing*, pp. 669-680. https://doi.org/10.1007/978-981-99-0085-5_54
- [15] Jaros, R., Koutny, J., Ladrova, M., Martinek, R. (2023). Novel phonocardiography system for heartbeat detection from various locations. *Scientific Reports*, 13(1): 14392. <https://doi.org/10.1038/s41598-023-41102-8>
- [16] Misra, I.S. (2023). An engineering approach of noninvasive detection and analysis of human heart sound for alarm generation. In *Human-Machine Interface Technology Advancements and Applications*, pp. 143-180.
- [17] Malik, A., Mandala, S., Pramudyo, M. (2023). Study of feature extraction method to detect myocardial infarction using a phonocardiogram. *Jurnal Media Informatika Budidarma*, 7(3): 1238-1246. <https://doi.org/10.30865/mib.v7i3.6442>
- [18] Aleidan, A.A., Abbas, Q., Daadaa, Y., Qureshi, I., Perumal, G., Ibrahim, M.E., Ahmed, A.E. (2023). Biometric-based human identification using ensemble-based technique and ECG signals. *Applied Sciences*, 13(16): 9454. <https://doi.org/10.3390/app13169454>
- [19] Sletta, Ø.S., Molinas, M., Kumar, M., Cheema, A. (2023). Classifying unsegmented phonocardiogram signals using cepstral, temporal, and wavelet scattering features. NTNU.
- [20] Imane, D., Lotfi, H.C., EL Houda, B.Y.N. (2023). Pathology cardiac monitoring study of the phonocardiogram signal. *Journal of Theoretical and Applied Information Technology*, 101(10): 3998-4013.
- [21] Riccio, D., Brancati, N., Sannino, G., Verde, L., Frucci, M. (2023). CNN-based classification of phonocardiograms using fractal techniques. *Biomedical Signal Processing and Control*, 86: 105186. <https://doi.org/10.1016/j.bspc.2023.105186>
- [22] Torre-Cruz, J., Canadas-Quesada, F., Ruiz-Reyes, N., Vera-Candeas, P., Garcia-Galan, S., Carabias-Orti, J., Ranilla, J. (2023). Detection of valvular heart diseases combining orthogonal non-negative matrix factorization and convolutional neural networks in PCG signals. *Journal of Biomedical Informatics*, 145: 104475. <https://doi.org/10.1016/j.jbi.2023.104475>
- [23] Patwa, A., Rahman, M.M.U., Al-Naffouri, T.Y. (2023). Heart murmur and abnormal PCG detection via wavelet scattering transform & a 1D-CNN. *arXiv preprint arXiv: 2303.11423*. <https://doi.org/10.48550/arXiv.2303.11423>
- [24] Ismail, S., Ismail, B., Siddiqi, I., Akram, U. (2023). PCG classification through spectrogram using transfer learning. *Biomedical Signal Processing and Control*, 79: 104075. <https://doi.org/10.1016/j.bspc.2022.104075>
- [25] Abburi, R., Hatai, I., Samanta, S., Jaros, R., Martinek, R., Babu, T.A., Babu, S.A. (2023). Adopting artificial intelligence algorithms for remote fetal heart rate monitoring and classification using wearable fetal phonocardiography. *Authorea Preprints*. <https://doi.org/10.36227/techrxiv.22561735.v2>
- [26] You, N., Han, L., Zhu, D., Song, W. (2023). Research on image denoising in edge detection based on wavelet transform. *Applied Sciences*, 13(3): 1837. <https://doi.org/10.3390/app13031837>
- [27] Nath, M., Srivastava, S. (2023). 4th order Shannon energy envelope approach for localization of S1 and S2 for early-stage detection of heart valve dysfunction. *Traitement du Signal*, 40(2): 479-490. <https://doi.org/10.18280/ts.400207>